ACS APPLIED MATERIALS & INTERFACES

Research Article

www.acsami.org

Hybrid Energy Harvester Consisting of Piezoelectric Fibers with Largely Enhanced 20 V for Wearable and Muscle-Driven Applications

Yiin-Kuen Fuh,*[,†] Jia-Cheng Ye,[‡] Po-Chou Chen,[†] Hsi-Chun Ho,[†] and Zih-Ming Huang[†]

[†]Department of Mechanical Engineering and [‡]Energy Engineering, National Central University, No.300, Jhongda Road, Jhongli District, Taoyuan City 32001, Taiwan, R.O.C.

Supporting Information

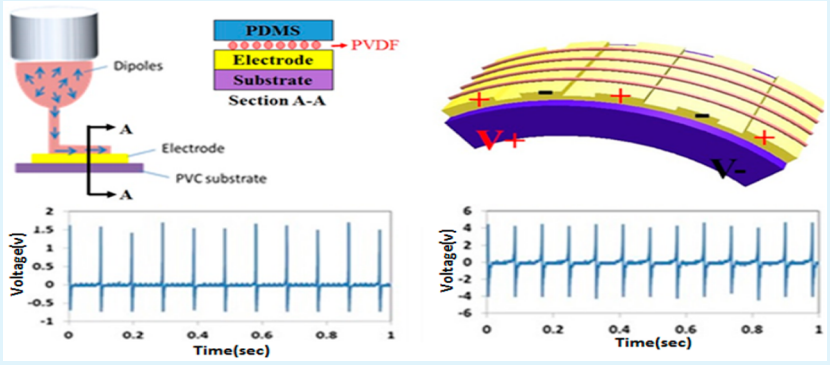

ABSTRACT: We present a polyvinylidene fluoride (PVDF) nanogenerator (NG) with advantages of direct writing and in situ poling via near-field electrospinning (NFES), which is completely location addressable and substrate independent. The maximum output voltage reached 20 V from the three layers piled NGs with serial connections, and the maximum output current can exceed 390 nA with the parallel integration setup. Linear superposition and switching polarity of current and voltage tests were validated by the authentic piezoelectric output. Nanofiber (NF)-based devices with a length ∼5 cm can be easily attached on the human finger under folding−releasing at ∼45°, and the output voltage and current can reach 0.8 V and 30 nA, respectively. This work based on NFs can potentially have a huge impact on harvesting various external sources from mechanical energies.

KEYWORDS: *near-field electrospinning, nanogenerator, energy harvester, nanofibers, polyvinylidene fluoride, muscle-driven*

INTRODUCTION

Renewable and nonexhaustible energy resources such as wave power and wind have rekindled considerable intensive interest to prevent global warming and dwindling resources. However, solar and thermal energies are highly dependent on time and location and are not universally ubiquitous and accessible. Therefore, human-motion-based energy harvesting has attracted tremendous interest due to the growing popularity of portable smart electronics as an independently self-sufficient and sustainable power source. Progress in nanogenerators (NGs) for portable electronics[1] and self-powered nanosystems has become more technologically feasible due to the advancement of extremely low power consumption nanoelectronics. Furthermore, harvesting energy from negligible human action or tiny body movement is very promising since it is location independent, especially for personal electronics, and human-based activities and associated mechanical movement are comparatively reliable and environmentally independent. The first significant contribution can be traced back to 2006: the piezoelectric zinc oxide (ZnO) nanowire (NW) arrays were demonstrated to convert tiny mechanical energy into electrical energy. To deflect aligned NWs by using a conductive atomic force microscope tip in contact mode and ∼8 mV, ∼0.5 pW were generated from a single NW actuation.[2] Furthermore, a scalable sweeping-printing method was proposed to fabricate stretchable and high output NGs; an open-circuit voltage up to 2.03 V, close-circuit current of 100 nA, and peak output power density of ∼11 mW/cm^3 were achieved.[3] Poly(vinylidene fluoride) (PVDF) is another alternative material for piezoelectricity and nanofibers (NFs) with diameters ranging from 70 to 400 nm produced by electrospinning. Domain switching and associated ferro-/piezoelectric properties of the electrospun PVDF fibers have shown well-defined ferroelectric and piezoelectric properties.[4] Considering the hybrid device consisting of a piezoelectric PVDF NF NG and a flexible enzymatic biofuel cell, the open-loop voltage of 15−20 mV and the short-circuit current of 0.2−0.3 nA were obtained.[5] Recently, near-field electrospinning (NFES) is proven to be able to achieve the direct-write capability to enable well-controllable ability and precise patterning to deposit substantial NFs in a continuous, direct-write, and controllable process.[6] Geometric patterns such as grid arrays and circular shapes on wide and flat areas can be reliably obtained[7] with well-controllable manner. In recent years,

Received: November 12, 2014
Accepted: July 3, 2015
Published: July 3, 2015

DOI: 10.1021/acsami.5b03955
ACS Appl. Mater. Interfaces 2015, 7, 16923−16931

rapid progress has been made on the fundamental mechanism of NF deposition via NFES such as controlled formation of multiple jets[8] and associated self-organization behavior based on the wave propagation theory.[9] For biocompatible material such as chitosan/poly(ethylene oxide), successfully direct-write and well-aligned NFs deposited in a continuous fashion were demonstrated.[10] For functional material such as piezoelectric PVDF, a comparative study utilizing both continuous near-field electrospinning (CNFES) and conventional electrospinning processes of electrospun PVDF-based membranes (EPMs) was also investigated in terms of fiber dimension, processing parameters, crystallinity, differential scanning calorimetry (DSC), Fourier transform infrared spectroscopy (FTIR), etc.[11] On the recent application of NFES, fabrication of monolithic polymer nanofluidic channels via NFES electrospun NFs as sacrificial templates was demonstrated, and 550−800 nm nanofluidic channels can be reliably fabricated based on this template method.[12] Another interesting area is for cell morphology and spreading control, and direct-write, highly aligned chitosan-poly(ethylene oxide) NF patterns are successfully demonstrated.[13] In addition, based on the NW and percolation theory, the ultralong metallic microwires were pursued to replace the brittle indium tin oxide (ITO), and a pattern transfer technique has been developed based on the process of an electrospun NF template, sputtered metallic layers, and soft stamp transfer of aligned metal nano/microwires as flexible transparent electrodes.[14] Applying the NFES technique as a viable tool to fabricate the NGs was initially pioneered, and a direct-write PVDF NG with high energy conversion efficiency was successfully demonstrated. Possibly owing to fewer defects of the NFES process and a higher degree of crystallinity, the electrical outputs of 0.5−3 nA and 5−30 mV for a single NF for the efficiency as high as 21.8% were achieved, as compared with the film counterpart of 0.5−4%.[15] In order to amplify the harvested energy, PVDF electrospun NFs arranged in a series and/or in parallel with patterned comb-shaped gold electrodes were also presented, and a peak current of 35 nA and peak voltage of 0.2 mV were measured.[16] Significant progress toward a usable output in the range of ∼V was newly made. The continuous deposition of PVDF NFs poses a strict challenge, and a restricted operating region was recognized, resulting in the massively parallel aligned nano/microfiber-based harvester fabricated via oriented and in situ poled NFES. The major advancement to aligned and oriented poled 500 microfibers deposited continuously in parallel and serial configurations is able to produce a peak output current of ∼300 nA and a voltage of ∼1.7 V, for which the magnitude increment is two to three orders in both current/voltage outputs when comparing the NFES setup of a single NF to the similar amount of nano/microfibers with post poling treatment.[17] For the integrated hybrid cell with various energy sources such as thermoelectric and solar cells, previously demonstrated mechanical harvesters are mainly focused on triboelectric nanogenerators (TENG), while the applications are self-powered sensors, water splitting without an external power source,[18] and energy storage in a Li-ion battery for lighting up LEDs.[19]

EXPERIMENTAL SECTION

In this paper, we demonstrate an in situ poled and direct-write NG via NFES process to massively fabricate PVDF NF arrays and fully encapsulated on a flexible substrate. Highly reproducible and integrated multiple NGs connected in serial and parallel are experimentally capable of increasing output voltage and current. In serial connections, the three-layer stacked NGs can reach a maximum output voltage of 20 V. Alternatively, the maximum output current 390 nA can be achieved from the parallel integration of the same device. The size of the fabricated NG was 3.5 cm × 1 cm × 2 μm. The electrical outputs (VL) are measured to be 4 V, while the power output reaches the optimized output power of 5.34 μW at matched resistance of 1.5 MΩ. The power density amount 7629 μW/cm^3 has been achieved. As a comparison, the generated power density is on a similar magnitude of previously published fiber-based generator and compared favorably with the MEMS-based counterpart.[9]

Finally, the muscle-driven capabilities of developed NG devices are also demonstrated for a fiber-based wearable technology and open up the potentially promising solution of harvesting the energy from human activity with minimal intervention. Moreover, a hybrid cell is demonstrated, which is capable of harvesting energy from tiny mechanical motions.

Figure 1(a) shows the schematic diagram of the direct-write and NFES PVDF fibers with in situ electrical poling and mechanical stretching steps. In the serial/parallel configuration, electrical voltage and current superposition can be accomplished effortlessly via the adjustment of the electrode gap distance. The mode of the deformation and the current/voltage scaling-up superposition principle for the electrospun NFs are integrated as one massive-array energy gathering apparatus. As mechanical deformation is applied onto the substrate, a corresponding piezoelectric potential in the NFs can be induced, where the "±" signs represent the polarity of the local piezoelectric potential created inside the NFs in situ. Figure 1(c,d) illustrates the schematic diagram of the electrode gap effect in serial (current) and parallel (voltage) configuration, respectively, suspending multiple fibers across two or more copper contact electrodes (made of 55 μm thick copper foil) on an insulation polyvinyl chloride (PVC) substrate deposited by the direct-write NFES process.[15] The typical electrode separation distance is in the range of 50−120 μm, and the direct-write technique is comprehended by using an x−y stage (Parker, Inc.) to control the deposition rate and course of the substrate during the NFES process, resulting in a desirable pattern at specific regions of interest. PVDF solution is prepared by using *N*,*N*-dimethylformamide (DMF) (Sigma-Aldrich) as solvent for PVDF powder (Sigma-Aldrich, Mw = 534 000), and acetone and fluorosurfactant (ZONYL UR) are added to optimize the evaporation rate and surface tension of the solution, respectively.[10] The electrospinning process parameters used in this case are 16 wt % PVDF, solvent (DMF:acetone with 1:1 weight ratio), 4 wt % fluorosurfactant (Capstone FS-66), 1.2 mm for the needle-to-collector distance, and 1.44 kV for the electrospinning voltage. The size of the fabricated NG was 3.5 cm × 1 cm × 2 μm. Encapsulation with PDMS was applied to secure structural stability.

In Figure 1(e,f) a total of about 500 parallel NFs were electrospun on top of the 10 and 40 metallic electrodes, respectively, with different working gaps, 120 and 50 μm, respectively which were between two electrodes. When dynamic strain/stress was applied by deforming the flexible substrate, there were about 5000 active working contacts for 10 metallic electrodes and 20 000 active working contacts for 40 metallic electrodes to harvest charges generated from these PVDF NFs. The as-spun PVDF NFs have average diameters ranging from 900 nm to 2.5 μm. Figure 1(g,h) investigates the performance of output voltage that can be greatly enhanced by superpositioning a number of electrode pairs in a series of configurations. The experimental results were obtained by measuring approximately 5000 rows and 20 000 rows of NF arrays, respectively. Then, a cyclic stretching−releasing deformation at a strain of 0.5% and 10 Hz by a linear motor was used to periodically deform the electrospun NG. For example, the NG output voltage was connected in a series, leading to an output voltage of 1.5 and 4 V when the substrate was stretched and released repeatedly. The corresponding AFM images were shown in Figure 1(i), indicating the diameter was ca. 2.5 μm, which is the average diameter of electrospun NFs. Previously, an experimental validation on the spinnability of NFES PVDF NFs was investigated and facilitated here such that the stable NFES spinning window of continuous and large-area deposition was reproducibly carried out.[17] However, the continuous deposition of PVDF NFs was identified as a limiting and pretty narrow operating region, at the sacrifice of diameter variation of NFs. We intentionally choose the most obviously different diameters of NFs and perform the characterization.

DOI: 10.1021/acsami.5b03955
ACS Appl. Mater. Interfaces 2015, 7, 16923−16931

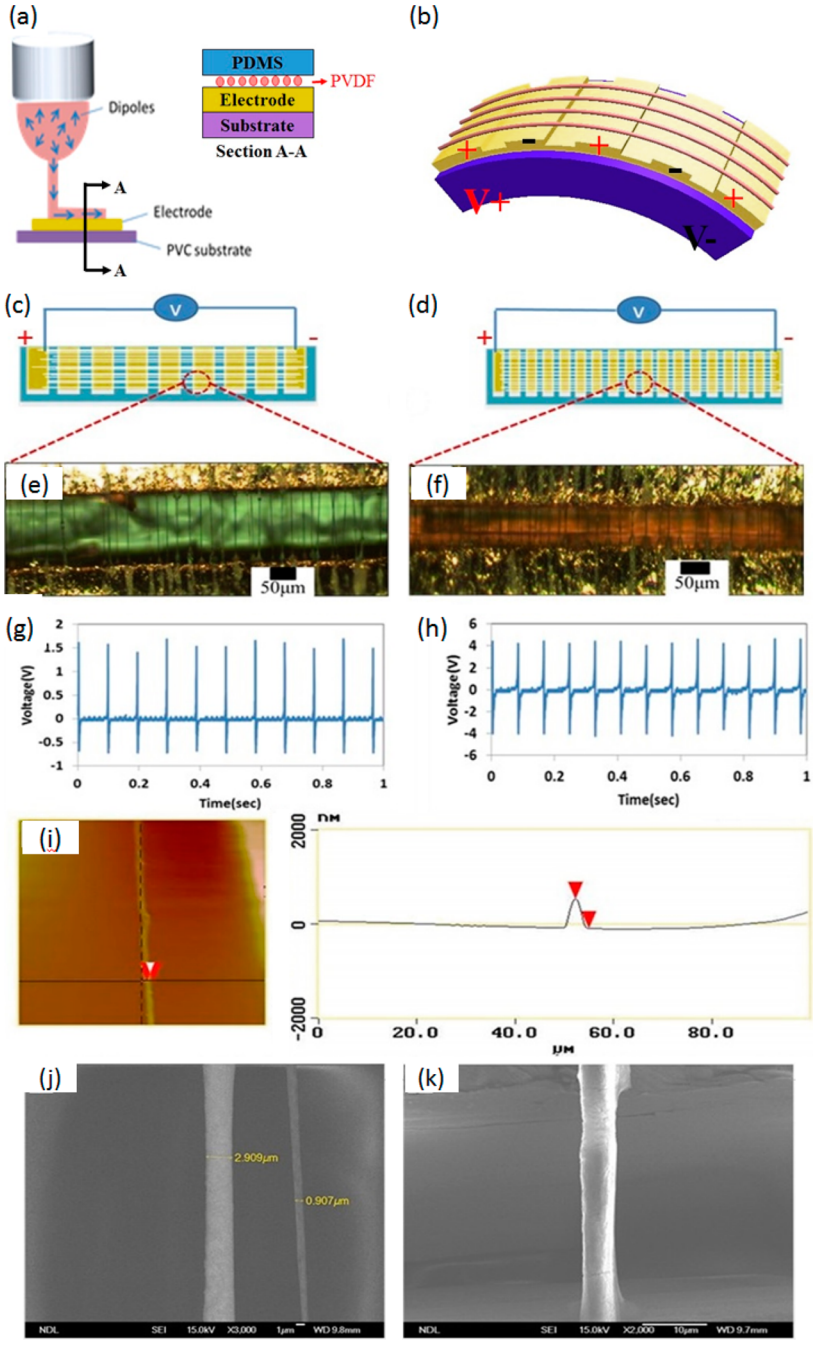

Figure 1. (a) Schematic of the in situ, direct-write, and electrical poling PVDF fibers via NFES. The mechanical stretching forced fibers deposited onto a flexible PVC substrate to construct the NG. (b) Mode of deformation schematic. When mechanical deformation was loaded on the substrate, a corresponding piezoelectric potential in the NFs can be elicited by the tensile strain, where the "±" signs indicate the polarity of the piezoelectric potential. (c,d) Schematic diagram of the NG design. Different electrode gap on the same flexible substrate, respectively, (e) A total of about 500 parallel NFs and 10 electrode pairs have been fabricated on top of a flexible substrate. (f) A total of about 500 parallel NFs and 40 electrode pairs have been fabricated on top of a flexible substrate. (g,h) According to the different electrode pairs, the output voltage of NG voltage superposition in serial configuration. (i) Atomic force microscope (AFM) images of PVDF nanofibers via direct-write NFES technique. (j) Scanning electron microscope (SEM) images of electrospun PVDF nanofibers of two different diameters fabricated via direct-write NFES manner. There are diameter variatiosn of NFs as shown at 0.9 and 2.9 μm, respectively. (k) Another zoomed SEM photomicrograph showing NFs with a diameter of ~4.8 μm.

The corresponding SEM images were shown in Figure 1(j) of two PVDF NFs fabricated sequentially via direct-write NFES processing conditions, indicating the diameter was ca. 2.9 and 0.9 μm, respectively. Figure 1(k) shows another fiber with diameter ca. 4.8 μm, which is one of the largest diameters, and the uniformity of electrospun fibers can be further improved by tightly controlling the processing conditions such as precise electric field via constant tip-to-electrode distance and solution conductivity, viscosity, as well as surface tension.

For the crystallinity characterization of PVDF NFES electrospun nanofibers and the related polarized phase, the spectroscopic evidence for the effective transformation from paraelectric to a high fraction of induced ferroelectric phase had been recently identified and proven.[20]

The key factors contribute to the highly efficient $\alpha \rightarrow \beta$ phase due to the oriented unit cells of hydrogen and fluoride (CH_2-CF_2) polar structure, and the β-phase is primarily responsible for PVDF's piezoelectric response. In order to largely enhance the β-phase PVDF, electrical

DOI: 10.1021/acsami.5b03955
ACS Appl. Mater. Interfaces 2015, 7, 16923−16931

poling and mechanical stretching processes are indispensable to directionally align the dipoles in the crystalline PVDF structures. Transformation has been found to be the indispensable step of mechanical stretching and electric poling processes during the NFES process as shown in Supporting Information Figure S1. A previously posed challenge on continuous deposition of PVDF nanofibers was overcome, and a pretty narrow operating region was identified[17] as shown in Supporting Information Figure S2. The spectroscopic evidence such as XRD and FTIR to demonstrate phase information on the produced NFs is shown in Supporting Information Figures S3 and S4, respectively. From the above data, the NFES direct-write electrospun PVDF fibers have these common phases (nonpolar α-phase and the polar β- and γ-phases) that were observed. Among these phases, the polar β-phase is the most important evidence of piezoelectric property.[20] We also tested the performance stability, besides process improvement. In Supporting Information Figure S5 the stability of NGs can be consistently observed.

RESULTS AND DISCUSSION

For the forward/reverse connection of voltage measurements, the positive/negative and negative/positive probes of the measurement system are connected to the positive/positive and negative/negative electrodes of the NG, respectively. The detailed experimental setup regarding the results presented in Figures 2−4 can be found in Figure S6 (Supporting Information). Considering the individual electrospun fiber, the piezoelectric coefficients have been characterized, and an average piezoelectric coefficient d_{33} of −63.25 pm/V was found, which is comparable to the previously reported values of NFES fibers[25] and is significantly larger than the PVDF thin films.[26−29] The detail of piezoelectric characterization can be found in Supporting Information Figure S7. In addition, we also did some simulations to obtain the piezoelectric coefficients of single poled PVDF fiber, and the results of the deformation of the PVDF fiber can be found in Supporting Information Figures S11 and S12.

Figure 2(a) shows the results for voltage output of one NG. The insets illustrate the corresponding connection configurations. As the NG is bent inward cyclically to induce the stretching states, corresponding positive peaks can be measured consistently. Similarly, when the substrate is released and the NG returns to a free state, a negative electric peak is concurrently measured. The mechanism with strain-induced piezoelectric potential and related electric signal generation can be found elsewhere.[15,17] The switching-polarity test is generally recognized to identify if the signal is an artifact or not, such that the true electricity output from the piezoelectric property of the NG can be proven. Experimentally, opposite polarities of voltage meter and NG are connected; i.e., the positive and negative probes of the voltage meter are connected to the negative and positive ends of the NG, respectively, as shown in Figure 2(b). The reversal output signal is experimentally measured as the stretching of the NG produces a negative pulse and vice versa. Additionally, the magnitude difference between the signal of forward connection and reverse connection is also observed in our NF-based NG, as similar phenomena were reported previously on zinc oxide (ZnO) NW-based NGs.[21] The electric current output of the NGs is presented in Figure 2(c),(d). In the same phase, in-synchronization of voltage and current output is observed such that a positive/negative current signal is generated when the NG is stretched/released. Figure 2(d) shows that the output current and switching polarity is also experimentally fulfilled. The inset at the bottom of Figure 2A,B illustrates the peak voltage which was measured to be ∼4 and ∼0.4 V in the forward and reverse connections, respectively. Similar to the voltage measurement, the current measurement result is plotted in Figure 2C,D. The polarity check for the piezoelectric response was confirmed since the shape of the response was flipped. The peak currents in the forward and reverse connections were ∼75 and ∼30 nA, respectively.

The capability of voltage scale-up can be demonstrated as the two NGs are serially connected as shown in Figure 3(a) and Figure 3(b). The superposition principle of voltage is satisfied when two NGs are connected in the same direction, as the final output can noticeably increase and basically follows the fundamental electric circuit theory. In comparison, the voltage output can be significantly reduced when two NGs are connected in opposite directions. In addition, the serially connected NGs must also meet the requirement of a switching-polarity test. On the other hand, the demonstration of full electrical signal superposition can only rely on the precise synchronization between two NGs such that the induced strain of either the deformed or released state should operate simultaneously. Any small off-synchronization or a little delay in the deformation will result in the distinctly different outputs of the two NGs. We experimentally demonstrate the phenomena of a pair of positive−negative peaks by oppositely connecting two serial NGs as shown in Figure 3(c). When two NGs are stretched or released in a fashion that one immediately follows the other, two NGs sequentially generated the double peak signals that are opposite in sign and slightly off-synchronized. In this case, NG B is bending first and follows the bending of NG A before the completion of NG B bending. This purposely off-synchronized implementation will result in the first double peak with a negative sign due to reversal connection. In what follows, the NG B releasing completion and the release of NG A, another peak with a positive sign is observed, in a fashion similar to the first double peak and reversal connection. Any measurement artifact and incompatibility of the linear superposition rule can be further validated as the two positive−negative peaks as presented in Figure 3(d). We also use the well-accepted method to characterize the true signals for output voltage and current of integrated NGs, and a linear superposition of either voltage/current can be satisfied for the two NGs in serial/parallel connection, respectively (Supporting Information Figures S8 and S9). Furthermore, the switching-polarity tests are also conformed for the two NGs, fully in agreement with published data, and indicate the true signals are obtained from the fabricated NGs.

For enhancing and scaling-up of both output voltage and current, the proposed direct-write, in situ poled NFES NGs can be effortlessly integrated in series and in parallel on a PVC substrate. To demonstrate the feasibility of scale-up in output voltage, NGs integrated serially with three layers on the PVC substrate, as shown in Figure 4(a), are used to characterize the electrical performance. We gradually increase the number of serially integrated layers and perform measurement sequentially to guarantee successful integration in serial.[22] The fabricated NF device is encapsulated in PDMS polymer on a PVC substrate as shown in Figure 4(b) of the optical image. We fabricate six units of NF-based generators, and one of the electrical outputs is measured to be 4 V and 75 nA, respectively, for voltage and current as shown in Figure 4(c). We also combine two units on the same structural layer to improve the output due to the simultaneously induced external force on the integrated layers in series. As such, the increment of output voltage was found due to the increasing number of layers via summing up the external piezoelectric potential. The voltage superposition can be distinctly demonstrated by serial integration as the output

DOI: 10.1021/acsami.5b03955
ACS Appl. Mater. Interfaces 2015, 7, 16923−16931

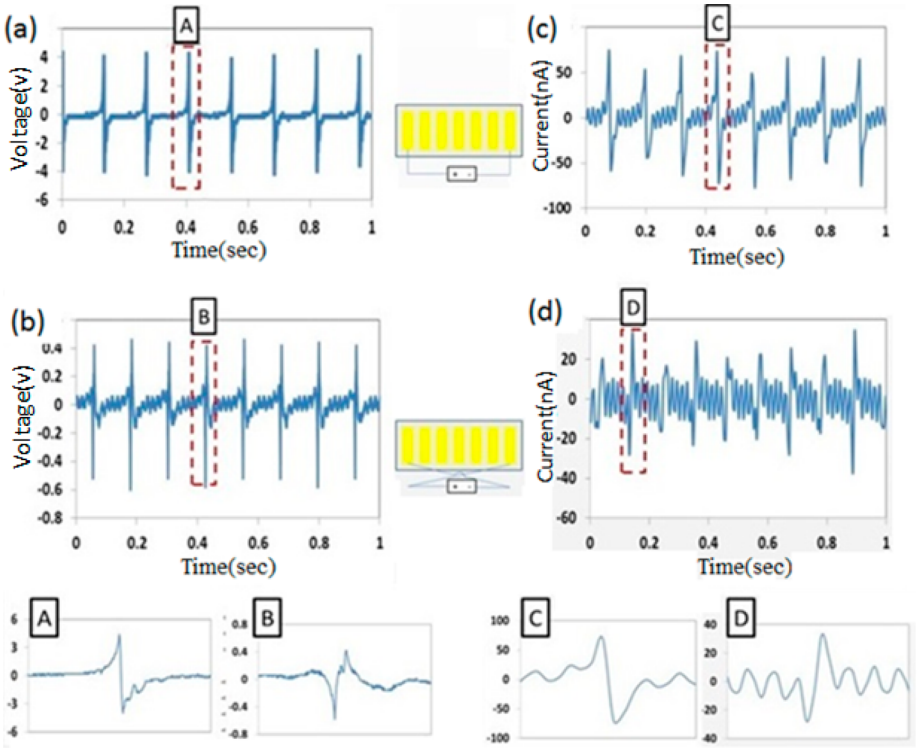

Figure 2. Polarity test under forward and reverse connections for (a, b) voltage output from NGs. (c, d) Current power output from NG. The magnified pattern of one single bending and release process is illustrated in the bottom plots A–D. Peak voltage was measured to be about 4 V in the forward connection and 0.4 V in the reverse connection, and the peak current was measured to be 75 nA in the forward connection and 30 nA in the reverse connection, respectively.

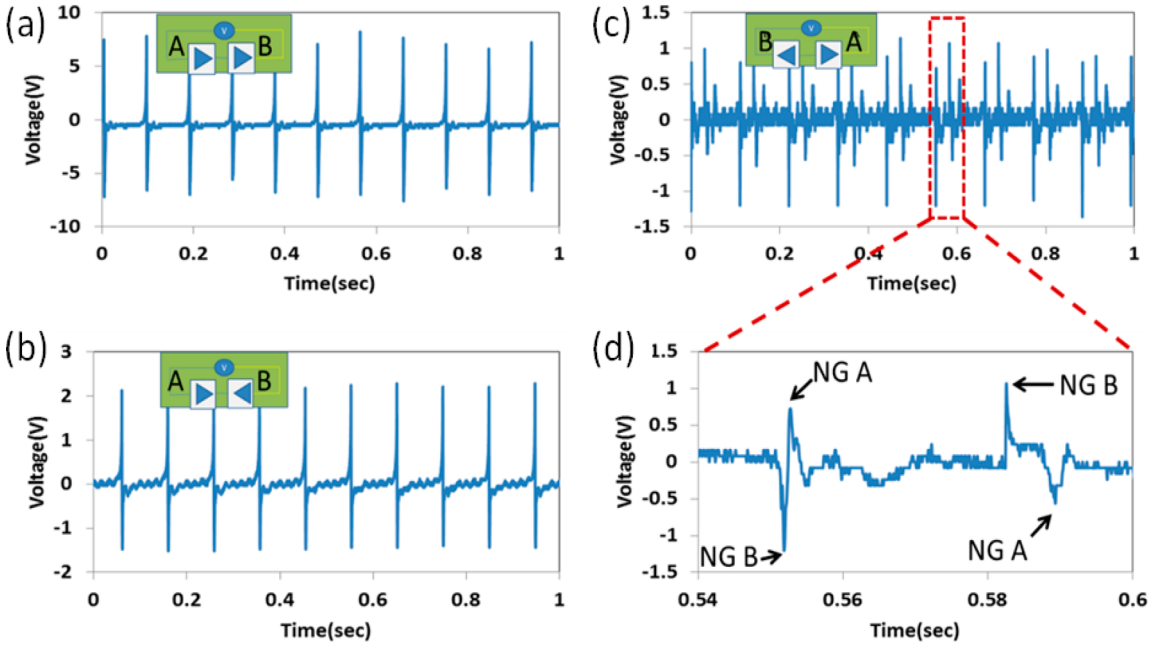

Figure 3. (a,b) Superposition of the voltage scale-up or cancellation effect is demonstrated in serial connection of NG A and NG B. The connection configurations of the NGs of all insets are in reference to the measurement system. (c) Intentionally deformed, the two NGs reversely connected in serial in a mode of slightly off synchronization and resulted in voltage output. The inset illustrates the connection configuration of the NGs. (d) Enlarged view of two outputs and double peaks in (c) to illustrate the abrupt switch in output voltage for NG A and B, respectively.

voltage increases with the number of serially integrated layers under the same conditions. As the number of integrated layers increases from 1 to 3, corresponding to a total of 6 units of NGs, their output voltages are effectively enhanced from 7.5 and 15 to 20 V, respectively. On the other hand, the output current enhancement can be achieved for the device integrated in parallel. For the layer of parallel integration, the measured output current is ~145 nA as shown in Figure 4(d). Concurrently integrated two- or three-layered NGs led to an increased output current of 260 and 390 nA, respectively, as shown in Figure 4(e,f). The superposition

DOI: 10.1021/acsami.5b03955
ACS Appl. Mater. Interfaces 2015, 7, 16923–16931

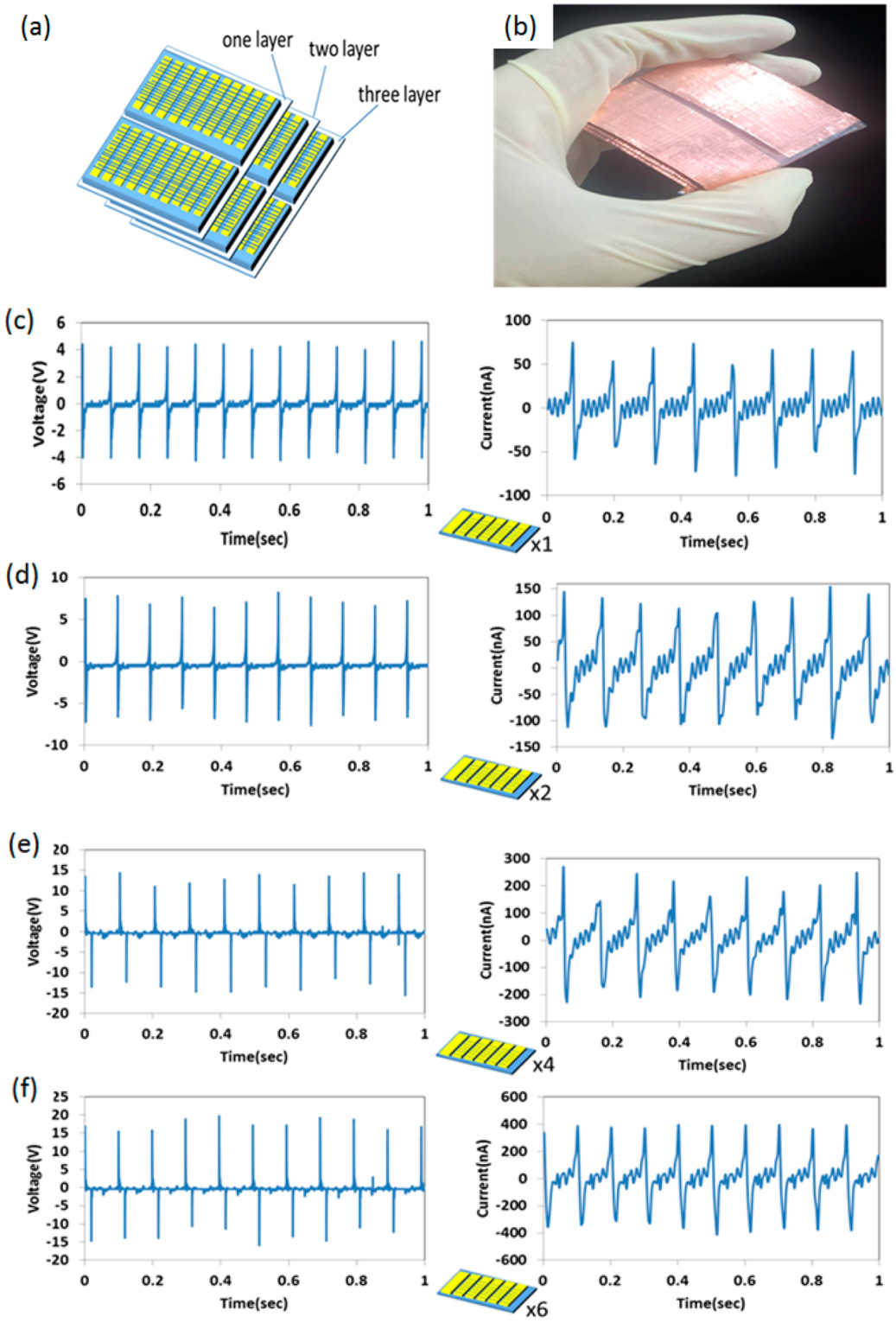

Figure 4. Largely enhanced electrical output NG device integrated in parallel for voltage and in serial for current. (a) Demonstration of the integrated NG to the feasibility of scale-up for promoting the output voltage and current. The number of integrated layers in the parallel and serial configurations is experimentally demonstrated to have a direct impact on the output voltage and current. (b) Photographic image of the NG device integrated in parallel and serial with three layers, i.e., six units of NGs. Output voltage and current of NGs integrated in serial and in parallel configuration, respectively, with (c) one unit, (d) one layer, (e) two layers, and (f) three layers. Please note that one layer in (d)−(f) contains two units of NGs.

demonstrated is not exactly the sum of the individual output in the measured series and parallel integrated NGs, and the reason may be attributed to variation in diameters of deposited NFs and successful deposition rate of individually fabricated NGs. Nonetheless, the direct-write, in situ poled, and large-area deposition as well as facile scale-up possibility of the series and parallel integration can be convincingly increased along with output voltage and current.

DOI: 10.1021/acsami.5b03955
ACS Appl. Mater. Interfaces 2015, 7, 16923−16931

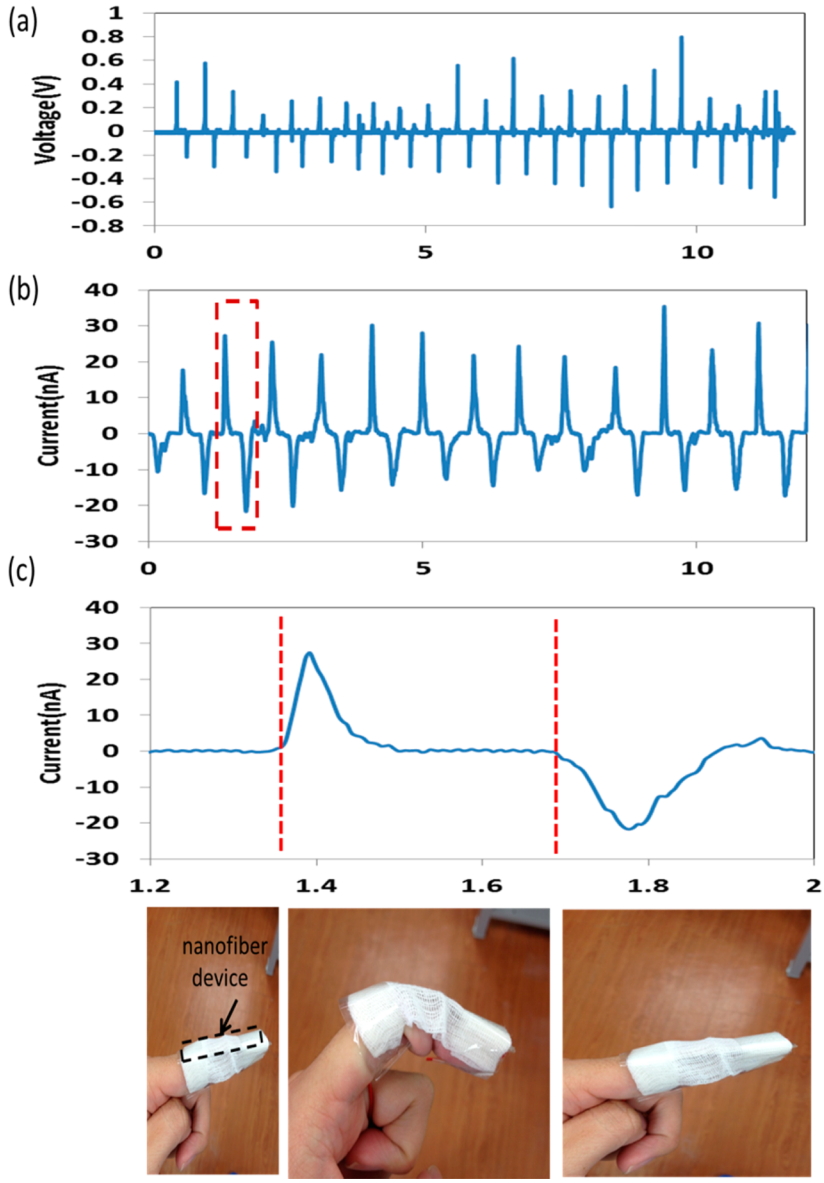

Figure 5. Human finger-enabled NG using direct-write, in situ poled NFs, and corresponding electrical measurements. The NF device is direct-write on the thin copper film with a predefined electrode pattern and fixed on textile substrate of woven cotton with dimension of 7.4 cm × 3.9 cm × 0.8 mm and mass density of 175 g/m^2, encapsulated with PDMS and attached on the finger. Experimentally, a uniform stress is induced as the finger folds and released during the measurements. (a) Multiple events of finger folding−releasing actions and corresponding voltage outputs of a NF device. (b) Current output of a NF device generated by bending and stretching out the finger. (c) A current output occurred on the event of the bending and stretching out action of the finger. The finger was held at an angle of ∼45°.

Wearable electronics self-powered from human activity such as walking and muscle movement are very promising as previously demonstrated.[23,24] Furthermore, structural 3-D spacers and functionally piezoelectric all-fiber textiles have also been developed as wearable NGs.[30] Here we demonstrate that our NF-based NGs can be easily deposited on the flexible textiles at a specific location with predefined electrodes and attached onto a human finger for scavenging the human movement. The encapsulated PDMS protecting layer is employed to prevent any undesired electrical noise from device contacts to the human skin directly. Our NF-based device exhibited the voltage and current outputs of ∼0.8 V and 30 nA, respectively, truthfully in-synchronized with the human finger motion, as shown in Figure 5(a,b). The bottom plots in Figure 5(c) show a firmly attached NF-based device on a finger and concurrently experience strain from the bending and stretching out actions of the finger. The novel structure of our NF-based device can be further improved by integrating another NFs-template transparent electrode[14] to achieve, in the field of wearable electronics, a completely flexible energy harvester that unnoticeably scavenges tiny mechanical activity of living creatures with very little obstruction.

Figure 6(a) and (b) shows the output performance of the fabricated NG and coin cell (Maxell, LR44,1.5 V/60 mAh), respectively. The corresponding output voltage is about 6.5 and 0.7 V, respectively. Figure 6(c) shows a schematic diagram of the hybrid energy cell with a bridge rectification circuit. Both the NG and the coin cell were connected for converting the alternating current to the direct current. Figure 6(c) shows the hybrid energy cell schematic of both the NG and the coin cell, where a full bridge rectification circuit was connected with the NG for

DOI: 10.1021/acsami.5b03955
ACS Appl. Mater. Interfaces 2015, 7, 16923−16931

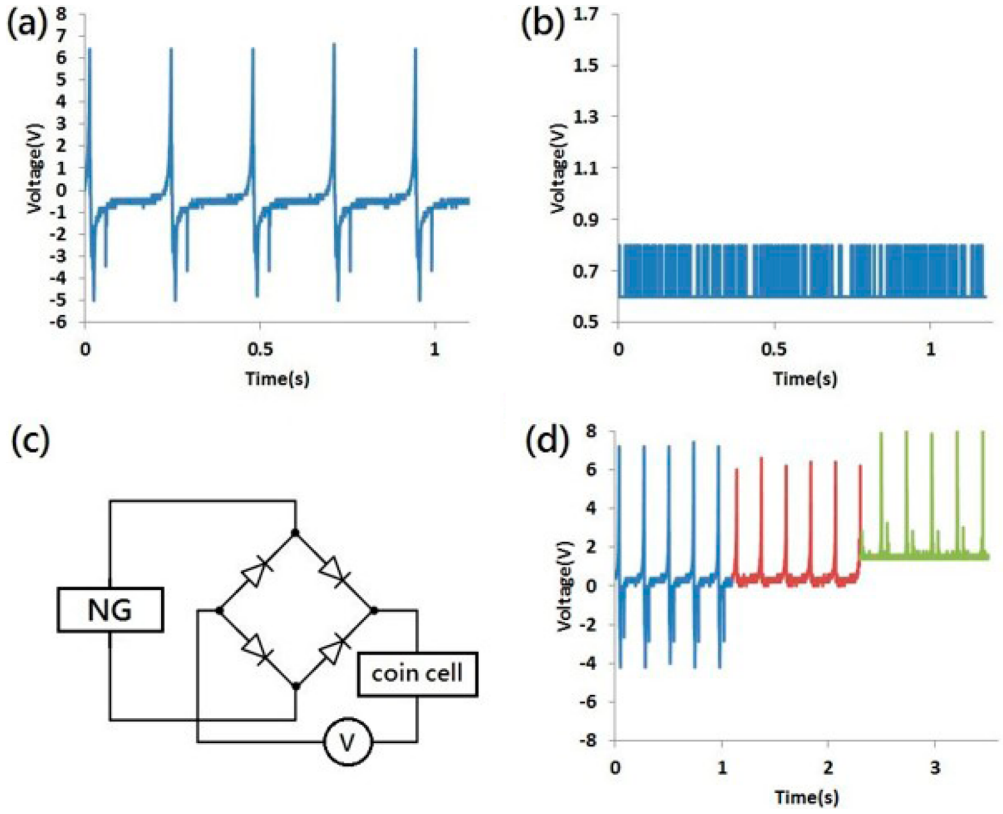

Figure 6. (a) Output voltage of NG with one layer of NF array in serial configuration. (b) Output voltage of coin cell. (c) Schematic diagram of the connection between the NG and the coin cell. (d) Output voltage of the hybrid coin cell and NG.

alternating current to direct current conversion. Figure 6(d) shows the output voltages of the NG before (blue) and after (red) rectification as well as the hybrid energy cell (green), respectively, in three different colors. It can be well demonstrated that the output voltage signals of the hybrid cell are rectified to be positive and much larger than the single energy harvester due to the superposition effect. In addition, we also scavenged the voltage and current of NGs with a two-layer NF array in serial configuration for the full rectification in Supporting Information Figure S10. Figure S10 shows the same result (positive voltage and current signals after rectified) but higher output power than NG with only one layer configuration.

CONCLUSION

Structurally robust, reproducibly scalable, substrate-independent, and large-area NGs utilizing the NFES direct-write technique to massively align piezoelectric PVDF NFs on flexible substrates have been successfully fabricated. The particular properties of in situ electrical poling and mechanical stretching can promise the scaling-up of the piezoelectric potentials with minimal effort to integrate NGs in parallel and/or series for improvement of output voltage and current. The NGs that comprised 20 000 rows of well-aligned PVDF NFs are able to create a peak output voltage of ∼4 V and a current reaching 75 nA. Furthermore, a highly promising and feasible power source for wearable electronics is demonstrated as the three-layer integrated NGs can reach the maximum output voltage and current up to 20 V and 390 nA, respectively. Two main contributions are summarized. First, the proposed device is 2 to 3 orders of magnitude increment in both voltage and current outputs when compared with either a single NF or similar NFES setup with post poling treatment due to opposite poling direction for a similar amount of NFs.[15] Second, by attaching our NF-based device (with a length of approximately ∼5 cm) on the human finger under folding−releasing at ∼45°, the output voltage and current can reach 0.8 V and 30 nA, respectively. In addition, we have also demonstrated an NF-based hybrid energy cell that can harvest mechanical energy. Therefore, this NF-based device and integrated hybrid cell can provide a highly promising renewable energy source for future wearable electronics that harvests the mechanical motion of humans with very minimal intervention.

ASSOCIATED CONTENT

Supporting Information

SEM, XRD, and FTIR of the fabricated device with parallel aligned NFs were performed and compared between the original PVDF powder, NFES PVDF fiber, and conventional electrospinning PVDF thin film. Deformation simulations of center displacement as a function of electric field were employed and compared with experimental measurements of various fiber diameters of single PVDF fiber such that the piezoelectric constant of deposited NFs can be deduced. The Supporting Information is available free of charge on the ACS Publications website at DOI: 10.1021/acsami.5b03955.

AUTHOR INFORMATION

Corresponding Author

*Tel.: +886-03-4267305 (office). Fax: +886-03-4254501. E-mail: michaelfuh@gmail.com.

Notes

The authors declare no competing financial interest.

DOI: 10.1021/acsami.5b03955
ACS Appl. Mater. Interfaces 2015, 7, 16923−16931

REFERENCES

(1) Wang, Z. L.; Zhu, G.; Yang, Y.; Wang, S.; Pan, C. Progress in Nanogenerators for Portable Electronics. *Mater. Today* **2012**, *15*, 532−543.

(2) Wang, Z. L.; Song, J. H. Piezoelectric Nanogenerators Based on Zinc Oxide Nanowire Arrays. *Science* **2006**, *312*, 242−246.

(3) Zhu, G.; Yang, R.; Wang, S.; Wang, Z. L. Flexible High-Output Nanogenerator Based on Lateral ZnO Nanowire Array. *Nano Lett.* **2010**, *10*, 3151−3155.

(4) Baji, A.; Mai, Y. W.; Li, Q.; Liu, Y. Electrospinning Induced Ferroelectricity in Poly(Vinylidene Fluoride) Fibers. *Nanoscale* **2011**, *3*, 3068−3071.

(5) Hansen, B. J.; Liu, Y.; Yang, R.; Wang, Z. L. Hybrid Nanogenerator for Concurrently Harvesting Biomechanical and Biochemical Energy. *ACS Nano* **2010**, *4*, 3647−3652.

(6) Sun, D.; Chang, C.; Li, S.; Lin, L. Near-Field Electrospinning. *Nano Lett.* **2006**, *6*, 839−842.

(7) Chang, C.; Limkrailassiri, K.; Lin, L. Continuous Near-Field Electrospinning for Large Area Deposition of Orderly Nanofiber Patterns. *Appl. Phys. Lett.* **2008**, *93*, 123111.

(8) Fuh, Y. K.; Hsu, H. S. Controlled Formation of Multiple Jets and Nanofibers Deposition Via Near-Field Electrospinning Process. *Int. J. Nonlinear Sci. Numer. Simul.* **2010**, *11*, 979−984.

(9) Fuh, Y. K.; Lien, L. C. Self-Organization of Multiple Jets in Near-Field Electrospinning Process. *Micro Nano Lett.* **2012**, *7*, 1088−1091.

(10) Fuh, Y. K.; Chen, S.; Jang, S. C. Direct-Write Well-Aligned Chitosan-Poly(Ethylene Oxide) Nanofibers Deposited Via Near-Field Electrospinning. *J. Macromol. Sci., Part A: Pure Appl.Chem.* **2012**, *49*, 845−850.

(11) Fuh, Y. K.; Lien, L. C.; Jang, S. C. A Comparative Study of PVDF Nanofibrous Membranes Prepared by Continuous Near-Field and Conventional Electrospinning Processes. *Micro Nano Lett.* **2012**, *7*, 376−379.

(12) Fuh, Y. K.; Hsu, H. S. Fabrication of Monolithic Polymer Nanofluidic Channels Via Near-Field Electrospun Nanofibers as Sacrificial Templates. *J. Micro/Nanolithogr., MEMS, MOEMS* **2011**, *10*, 043004.

(13) Fuh, Y. K.; Chen, S.; He, Z. Direct-Write Highly-Aligned Chitosan-Poly(Ethylene Oxide) Nanofiber Patterns for Cell Morphology and Spreading Control. *Nanoscale Res. Lett.* **2013**, *8*, 97.

(14) Fuh, Y. K.; Lien, L. C. Pattern Transfer of Aligned Metal Nano/Micro Wires as Flexible Transparent Electrodes Using An Electrospun Nanofibers Template. *Nanotechnology* **2013**, *24*, 055301.

(15) Chang, C.; Tran, V. H.; Wang, J.; Fuh, Y. K.; Lin, L. Direct-Write Piezoelectric Polymeric Nanogenerator With High Energy Conversion Efficiency. *Nano Lett.* **2010**, *10*, 726−731.

(16) Chang, J.; Lin, L. Large Array Electrospun PVDF Nanogenerators on A Flexible Substrate. *Transducers* **2011**, 747−750.

(17) Fuh, Y. K.; Chen, S. Y.; Ye, J. C. Massively Parallel Aligned Microfibers-Based Harvester Deposited Via in Situ, Oriented Poled Near-Field Electrospinning. *Appl. Phys. Lett.* **2013**, *103*, 033114.

(18) Yang, Y.; Zhang, H.; Lin, Z.-H.; Liu, Y.; Chen, J.; Lin, Z.; Zhou, Y. S.; Wonga, C. P.; Wang, Z. L. A Hybrid Energy Cell for Self-Powered Water Splitting. *Energy Environ. Sci.* **2013**, *6*, 2429−2434.

(19) Yang, Y.; Zhang, H.; Chen, J.; Lee, S.; Hou, T.-C.; Wang, Z. L. Simultaneously Harvesting Mechanical and Chemical Energies by A Hybrid Cell for Self-Powered Biosensors and Personal Electronics. *Energy Environ. Sci.* **2013**, *6*, 1744−1749.

(20) Lei, T.; Cai, X.; Wang, X.; Yu, L.; Hu, X.; Zheng, G.; Lv, W.; Wang, L.; Wu, D.; Sun, D.; Lin, L. Spectroscopic Evidence for A High Fraction of Ferroelectric Phase Induced in Electrospun Polyvinylidene Fluoride Fibers. *RSC Adv.* **2013**, *3*, 24952−24958.

(21) Yang, R.; Qin, Y.; Lin, C.; Dai, L.; Wang, Z. L. Characteristics of Output Voltage and Current of Integrated Nanogenerators. *Appl. Phys. Lett.* **2009**, *94*, 022905.

(22) Lee, S.; Hong, J.; Xu, C.; Lee, M.; Kim, D.; Lin, L.; Hwang, W.; Wang, Z. L. Toward Robust Nanogenerators Using Aluminum Substrate. *Adv. Mater.* **2012**, *24*, 4398−4402.

(23) Lee, M.; Chen, C.-Y.; Wang, S.; Cha, S. N.; Park, Y. J.; Kim, J. M.; Chou, L.-J.; Wang, Z. L. A Hybrid Piezoelectric Structure for Wearable Nanogenerators. *Adv. Mater.* **2012**, *24*, 1759−1764.

(24) Lee, S.; Bae, S.-H.; Lin, L.; Yang, Y.; Park, C.; Kim, S.-W.; Cha, S. N.; Kim, H.; Park, Y. J.; Wang, Z. L. Super-Flexible Nanogenerator for Energy Harvesting from Gentle Wind and as An Active Deformation Sensor. *Adv. Funct. Mater.* **2013**, *23*, 2445−2449.

(25) Pu, J.; Yan, X. J.; Jiang, Y. D.; Chang, C.; Lin, L. W. Piezoelectric Actuation of Direct-Write Electrospun Fibers. *Sens. Actuators, A* **2010**, *164*, 131−136.

(26) Dargaville, T. R.; Celina, M.; Chaplya, P. M. Evaluation of Piezoelectric PVDF Polymers for Use in Space Environments. Part I: Temperature Limitations. *J. Polym. Sci., Part B: Polym. Phys.* **2005**, *43*, 1310−1320.

(27) Ye, Y.; Jiang, Y.; Wu, Z.; Zeng, H. Phase Transitions of Poly(Vinylidene Fluoride) Under Electric Fields. *Integr. Ferroelectr.* **2006**, *80*, 245−251.

(28) He, X.; Yao, K. Crystallization Mechanism and Piezoelectric Properties of Solution-Derived Ferroelectric Poly(Vinylidene Fluoride) Thin Films. *Appl. Phys. Lett.* **2006**, *89*, 112909.

(29) Guthner, P.; Ritter, T.; Dransfeld, K. Temperature Dependence of The Piezoelectric Constant of Thin PVDF and P(VDF-TrFE) Films. *Ferroelectrics* **1992**, *127*, 7−11.

(30) Soin, N.; Shah, T. H.; Anand, S. C.; Geng, J.; Pornwannachai, W.; Mandal, P.; Reid, D.; Sharma, S.; Hadimani, R. L.; Bayramol, D. V.; Siores, E. Novel "3-D Spacer" All Fibre Piezoelectric Textiles for Energy Harvesting Applications. *Energy Environ. Sci.* **2014**, *7*, 1670−1679.

DOI: 10.1021/acsami.5b03955
ACS Appl. Mater. Interfaces 2015, 7, 16923−16931